

PACS numbers: 07.60.Dq; 07.68.+m
DOI: 10.1070/QE2010v040n07ABEH014288

Measurement of the surface wavelength distribution of narrow-band radiation by a colorimetric method

A.V. Kraiskii, T.V. Mironova, T.T. Sultanov

Abstract. **A method is suggested for determining the wavelength of narrow-band light from a digital photograph of a radiating surface. The digital camera used should be appropriately calibrated. The accuracy of the wavelength measurement is better than 1 nm. The method was tested on the yellow doublet of mercury spectrum and on the adjacent continuum of the incandescent lamp radiation spectrum. By means of the method suggested the homogeneity of holographic sensor swelling was studied in stationary and transient cases.**

Keywords: *colorimetry, wavelength measurement, digital camera.*

In dealing with holographic sensors it is necessary to know the degree of holographic layer swelling at different points [1–3]. The sensor is a Denisyuk hologram made by a laser in a hydrogel polymer matrix. Such a structure efficiently reflects light at a wavelength that is the double period of interference layers. Thus, by measuring the position of the maximum in the reflection spectrum one can find the period of the interference layers. The matrix contains specific chemical groups, which make it sensitive to the solution parameters (for example, to medium acidity) or to certain substances (for example, glucose). The substance makes the matrix shrink or swell, which changes the distance between the layers of scattering particles. This results in the fact that the hologram illuminated by white light reflects radiation at a changed wavelength. If the hologram structure is homogeneous when the reflecting layers are distributed uniformly and their number N is sufficiently large then the reflected radiation occupies a narrow spectrum band. If the reflection is weak (i.e., the transmission is close to unity) one can easily derive the expression that combines the efficient optical thickness D of the holographic layer with the spectral half-height width $\delta\lambda$ of the reflected radiation: $\delta\lambda = 0.886\lambda^2/(2nD) = \lambda/N$, where n is the refractive index for emulsion. At the hologram width 10 μm, refractive index 1.33, wavelength 550 nm (in this case, $N \sim 55$), the spectral width is approximately 10 nm.

Hence, the problem is reduced to the following. Assume there is a set of emitters on a plane. We are interested in obtaining the spectra of each emitter preferably simultaneously. It is not easy especially if the sources are closely packed and produce almost continuous radiating surface. The situation is simpler if radiation from each point is spectrally narrow. Then, the distribution of the average radiation wavelength over the surface can be found by the colorimetric method. At each surface point one should determine with the required resolution the magnitudes of three components of a colour vector, i.e., obtain a colour image of the surface under study. Presently, the solution of this problem by using digital devices has no principal difficulties. The aim of our work is to solve the problem by means of conventional digital cameras. Each pixel of the colour image presents a particular colour vector in the RGB system. In order to find the distribution of the average wavelength from the image it is necessary to know how the particular digital camera represents radiation of different wavelengths.

The colorimetric method [1] suggested for finding this distribution is as follows. Radiation passes to at least two detecting channels differing in spectral sensitivity. If in a certain spectral range (call it the working range) the ratio of spectral sensitivities of at least two channels is monotonous then one can determine the average wavelength of narrow-band radiation from the signal ratio in the channels (see Fig. 1). At the selective sensitivity of the ith channel $S_i(\lambda)$ its signal is $I_i = \int \mathrm{d}\lambda S_i(\lambda)\Phi(\lambda)$, where $\Phi(\lambda)$ is the source brightness. For the δ-shape spectral source with brightness Φ_0, which emits at the wavelength λ_x, the signal in this channel is $I_i = \Phi_0 S_i(\lambda_x)$. If the ratio of the spectral sensitivities for two chosen channels is $\alpha(\lambda)$, then the sought-for wavelength is the solution of the equation $\alpha(\lambda_x) = I_1/I_2$:

$$\lambda_x = \alpha^{-1}(I_1/I_2),$$

where α^{-1} is the function inverse to $\alpha(\lambda)$. If the sought-for wavelength is outside the working range, i.e., outside the range

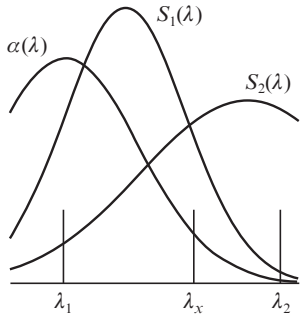

Figure 1. Qualitative view of the spectral sensitivities $S_1(\lambda)$ and $S_2(\lambda)$ of working channels and their ratio $\alpha(\lambda)$; λ_1 and λ_2 are the limits of working range, λ_x is the wavelength of a monochromatic radiation source.

A.V. Kraiskii, T.V. Mironova, T.T. Sultanov P.N. Lebedev Physics Institute, Russian Academy of Sciences, Leninsky prosp. 53, 119991 Moscow, Russia; e-mail: kraiski@sci.lebedev.ru

Received 29 January 2010; revision received 27 May 2010
Kvantovaya Elektronika **40** (7) 652–658 (2010)
Translated by N.A. Raspopov

of monotonous ratio of sensitivities in two channels, then the unique wavelength determination necessitates an additional (third) channel.

The case of a finite spectral width is not as simple as that of a δ-like source. In our case the spectrum of reflection from a holographic layer may widen due to several reasons. First, due to a small number of efficiently reflecting layers, which can be related either to a small thickness of the holographic layer or to a short depth of radiation penetration into the layer because of the high reflection caused by high amplitude of the variable part of refractive index or by strong scattering of light. Second, the spectrum may widen due to the nonuniform periodicity of layers in depth. We are interested in layer swelling, which is a reason for period variations and is related to the position of reflection maximum. In the latter case it is important to find the average period of layers, which is related to some average wavelength. Obviously, at moderate broadening this parameter can also be determined by means of the procedure described above using the signal relation in different spectral channels. However, in the general case the period obtained in this way from the position of maximum in the measured reflection spectrum differs from the average period. The difference depends both on a particular shape of reflection spectrum and on spectral sensitivities of the channels. The criterion for acceptable line broadening should be the permissible distinction of determined average period from its actual average value. If the sensitivity of sensors is almost constant within the line width of radiation illuminating a single pixel of the array, then radiation actually behaves as monochromatic one. If the spectral sensitivities of the sensor linearly vary within the width of the line that is symmetrical in shape, then the average period determined is the same as that in the case of a monochromatic source. If this condition is ruled out, then in the general case the determined wavelength is distinct from average one.

The possibility of measuring the wavelength of narrow-band radiation by a set of sensors was considered in the literature. However, only the problems of their different spectral sensitivities were discussed [4, 5]. Here, we consider the employment of digital cameras available and methods for obtaining reliable information on the distribution of the average wavelength over the source surface by its digital photograph rather than possible creation of a new device.

In the general case, the colorimetric measurements imply a projection of the surface under study to the detecting array through two (or, for expanding the range, a greater number) types of light filters, i.e., it is necessary to create a colorimetric device with a sufficient spatial resolution. A digital camera is just such a device.

In Fig. 2, the spectral sensitivities are shown for three types of eye cones responsible for colour recognition [6]. A digital camera also distinguishes colours but the spectral sensitivity of its sensors is distinct. For example, we will show below that in the spectral range 540–575 nm a digital camera does not discriminate different colour hues at all.

In Fig. 3, the signals of red (R), green (G), and blue (B) sensors of a Sony 717 digital camera are shown that were obtained from a digital photograph of the incandescent lamp spectrum. The spectrum was detected from a spectrograph with a diffraction grating (~ 800 lines mm^{-1}). This and all the following results were obtained at the sensitivity ISO 100 and switched-off automatic white balance. If the emission spectrum under study fits one of the two marked working ranges then the digital camera is appropriate for measurements. Note that

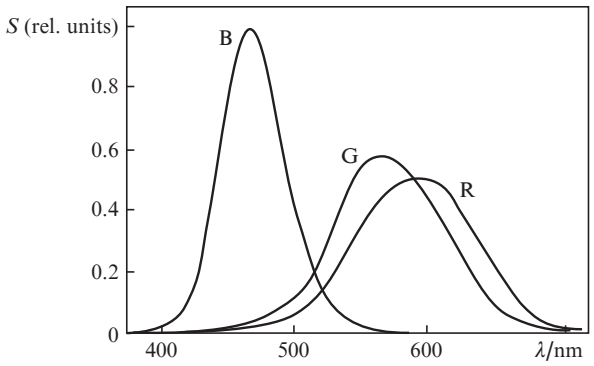

Figure 2. The spectral sensitivity of the human eye: signals of red (R), green (G), and blue (B) receptors [6].

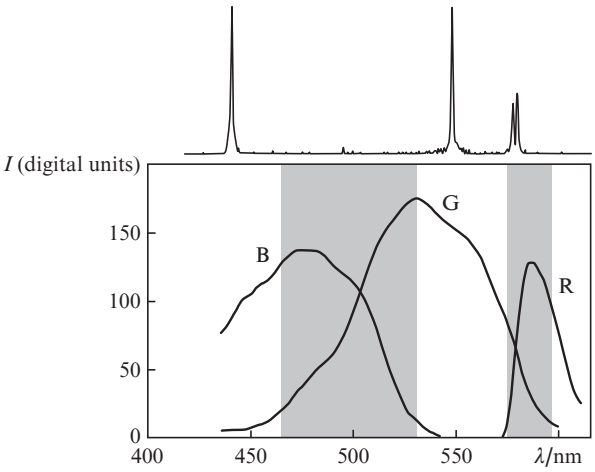

Figure 3. The spectrum of the mercury lamp (top) and signals of red (R), green (G), and blue (B) sensors obtained from the photograph of the incandescent lamp spectrum taken by a colour digital camera (bottom). The working wavelength ranges are marked.

we studied about ten various cameras and have found that their sensor characteristics are qualitatively similar. Figure 4 shows how a continuous spectrum (colour hue) is represented by digital cameras of various brands. Nevertheless, we did not study the characteristics of particular cameras as we wanted to understand the situation as a whole. Only the basic working Sony 717 digital camera was thoroughly studied. The

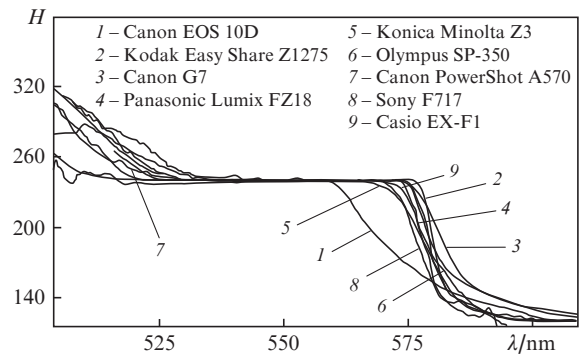

Figure 4. The colour hue H versus wavelength for some digital camera types.

spectrum of the incandescent lamp with an added calibrating spectrum of the mercury lamp was photographed. The shots used for the comparison were not overexposed, i.e., the maximal signal amplitude in channels was not above 150–200 digital units (the maximal admissible signal is 255 digital units).

The colour hue H was determined in a standard way as the polar angle in the cylindrical coordinate system of a three-dimensional colour space. Its value was from 0 to 360. For convenient work in red, green, and blue colour ranges we chose the reference point for the colour hue in the blue range ($H = 0$ at R = 0, G = 0, B = 255). In this case, the break of the colour hue (0–360) fits the blue range and introduces no additional difficulties in data processing. The purely red colour (R = 255, G = 0, B = 0) corresponds to $H = 120$ and purely green colour (R = 0, G = 255, B = 0) corresponds to H = 240. A more thorough analysis of various digital cameras is interesting but is beyond the framework of the present paper. Anyway, some general information may be obtained from Fig. 4. The principal conclusion important for our work is that all the digital cameras used have a defect of colour sensitivity in the green range.

Some modern cameras provide the possibility for extracting unprocessed data in the RAW format. Preliminary experiments show that the situation with the colour sensitivity in this case is better. The processor of the digital camera does not distort data but further investigations are necessary for using the RAW format. At the first stage, we limited our study to simplest (mass) formats (JPEG, BMP) by the following reasons. Creation of holographic sensors was assumed admass and our aim was to develop not only a simple method for checking the quality of sensors but for reading data from them also. The method should be available for mass users, i.e., should rely on simplest digital cameras, in which the RAW format is not presented now. In addition, the processing of the image of the holographic sensor surface should be maximum simple.

A particular procedure for camera spectral calibration was developed because the responses of the three sensor types of the detecting array intricately depend not only on the radiation wavelength but on the exposure as well. The camera to be calibrated takes shots of a continuous spectrum superimposed on the mercury lamp spectrum with various exposures. Then, this spectrum is used for calibrating each image with respect to the wavelength (see Fig. 5). The images calibrated in this way are then processed together. The result is information on the relationship between the wavelength and sensor responses.

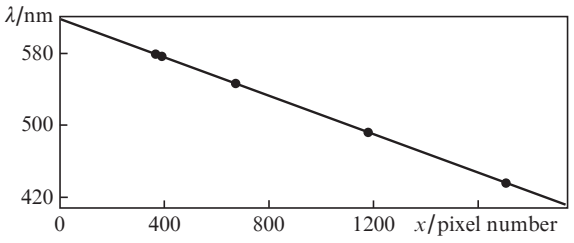

Figure 5. The calibration curve of the digital camera shows the relation between the wavelength of the incandescent lamp radiation spectrum and the horizontal coordinate (pixel number) of a shot. The points mark the mercury emission wavelengths used for the calibration.

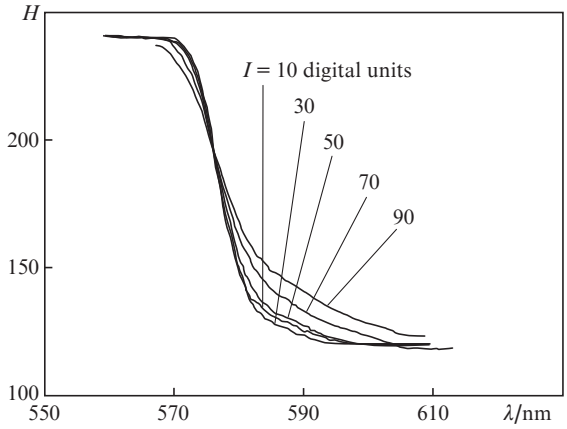

Figure 6. Colour hue of the obtained image versus radiation wavelength at various average signal magnitudes I.

In Fig. 6, the image colour hue is shown versus the radiation wavelength at various average signals I in grey gradations at each image point. The average signal is a third of the sum of the signals from the three colour channels. One can see that at various I the same wavelength may correspond to different colour hues of the obtained image. This concerns not only overexposed shots (the colour in the limiting case R = 255, G = 255, B = 255 is lost) but shots with a normal exposure as well.

In Fig. 7, the signals in green and red channels of the sensitive array and the colour hue for Sony F717 are shown versus I at fixed wavelengths. The range 570–605 nm is considered in which the red and green sensors are sensitive. The signal in the blue channel in this range is not above the noise level. One can see that with increasing the average signal I the sensor signals grow nonlinearly, their behaviour noticeably depending on the wavelength. As a consequence, the colour hue changes with increasing I. Near the range boundaries (see Figs 7a and f) with increasing I a threshold-like effect is observed: the response of the sensor with low sensitivity in this domain only arises at a certain magnitude of I.

On the basis of all the obtained dependences the characteristic surface is plotted for the camera under study, which gives the sought-for wavelength as a function of the colour hue and the average value of I (see Fig. 8). Once the characteristic surface is plotted the camera can be used as a spectral device in the working range of wavelengths and sensor responses. Applicability of the method was verified on the yellow doublet of the mercury spectrum and on a continuous spectrum of the incandescent lamp (see Fig. 9).

Having processed the image of spectrum (in Fig. 9a, the domain is shown fitting the working wavelength range) we obtain the map of the wavelength distribution over the image (Fig. 9b); only the image domains from the processing system working range are taken into account. Domains with too low values of I, in which the signal is close to noise, are neglected. Also neglected are the domains with high I in which, probably, noticeable redistribution of signals over different colour channels occurs and domains with almost a zero sensitivity of one of the two sensors. This explains the complicated contour of the wavelength distribution map over the image in the continuous spectrum range. It is interesting that due to different intensities of sources one can see in Fig. 9a the domain with superimposed continuous spectrum and mercury lines. On the wavelength distribution map there is no such superimposed

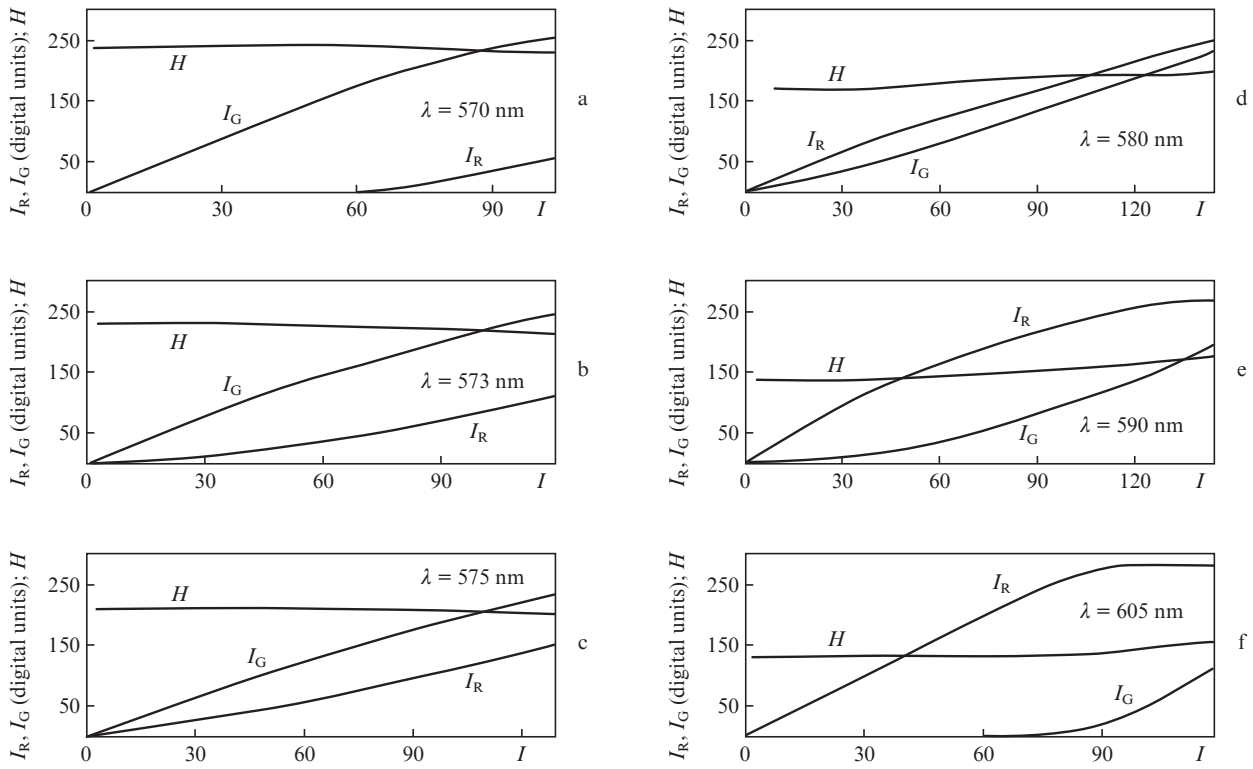

Figure 7. Signals in green and red channels and colour hue versus the average signal I at fixed wavelengths.

domain, which proves that the recovered wavelengths are equal despite the different intensities. In Figs 9c and d the distributions of various characteristics are shown for horizontal cross sections of the image. It is known that a spectral device with a diffraction grating has a linear dispersion (see Fig. 5), i.e., the wavelength should linearly vary with the coordinate (Fig. 9d), whereas the colour hue changes nonlinearly (Fig. 9c). The distribution columns (Figs 9e, f, g, and h, i, j) correspond to vertical cross sections of the image along the yellow doublet lines. In Figs 9e and h, the responses of red and green sensors are presented varying along the coordinate in a vertical cross section according to changing I. The colour hue also varies despite the constant wavelength (Figs 9f, i). Nevertheless, in vertical cross sections of the wavelength distribution map coinciding with the mercury spectrum lines (579 nm and 577 nm) the recovered wavelength is constant to a high accuracy both in the domain of mercury lines and in continuous spectrum (Figs 9g and j).

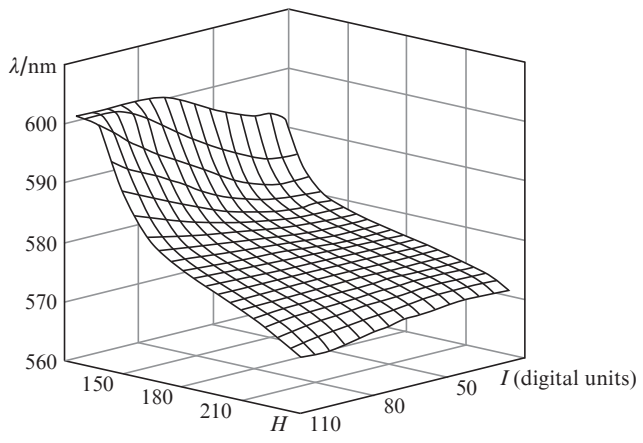

Figure 8. The characteristic surface for the Sony F717 digital camera. The detectable wavelength range 570–600 nm is in the sensitive region for red and green sensors.

By the digital image of the mercury spectrum for the yellow doublet lines and for underlying continuous spectrum we determined the standard deviation of the recovered wavelength in the limits of a narrow window oriented along the central (with respect to the spectrum) part of the mercury line. The window width was 4 pixels, which was less than the line width. The window height was 350 pixels and covered almost all the image of the mercury line and the whole corresponding part of the continuous spectrum. For the mercury doublet lines the wavelengths of 577 nm (the standard deviation is 0.16) and 579 nm (the standard deviation is 0.19) were obtained.

Note that in the case of the mercury spectrum image and continuous spectrum of the incandescent lamp each pixel is illuminated by an almost monochromatic light source, because the fraction of the continuous spectrum per single pixel of the image is less than 1 nm.

The developed method was employed for studying holographic sensors. The results are shown in Figs 10–13. The spectrum of radiation reflected from a holographic sensor is wider and the problem of possible inaccuracy in determining the wavelength requires particular investigations. One should keep in mind that in using holographic sensors it is important to know the shift of the wavelength under the action of solution surrounding the sensor rather than the absolute value of the wavelength itself.

Data presented in Figs 10 and 11 refer to a transient process. The hologram initially reflecting in the red range was

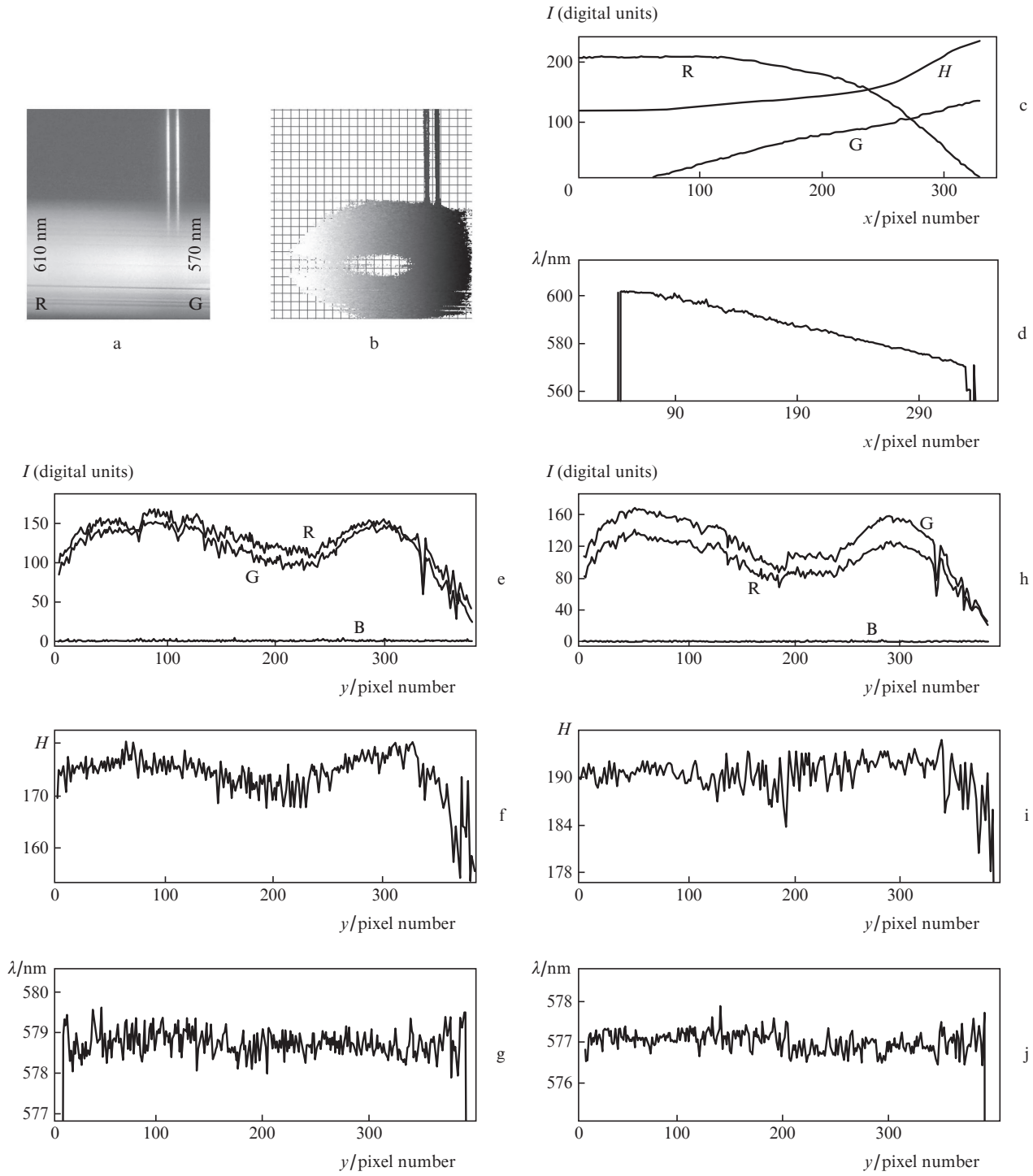

Figure 9. Illustration for an operating test of the method. Shot of spectrum fragment (a); the map of wavelength distribution over the image (b); the distribution of signals in red (R) and green (G) channels and colour hue (H) in a horizontal cross section of the shot (c); the horizontal cross section of the wavelength map (d); the distribution of signal in colour channels (e, h), colour hue (f, i), and calculated wavelengths (g, j) in a vertical cross section of the shot along the mercury doublet lines 579 nm (e, f, g) and 577 nm (h, i, j). A rectangular hatch on the wavelength map marks the domains in which the signals are beyond the working range and, hence, are excluded from calculation.

placed to a solution in which it contracted. The contraction is a sufficiently long process. From Figs 10 and 11 it is seen that from the boundaries to centre the wavelength as a whole varies from 580 nm to 598 nm, i.e., the wavelength spread is sufficiently large. This is an indication to inhomogeneous contraction of the hologram, the process being faster near the boundaries. The wavelength spread is also large in a small domain near each distribution point, which testifies that the deformation of the polymer matrix net of this sensor is not spatially uniform.

Data shown in Figs 12 and 13 correspond to a stationary state of the holographic sensor. In Fig. 12, the wavelength distribution map is shown calculated from a colour digital image of the holographic sensor surface. Two cross sections

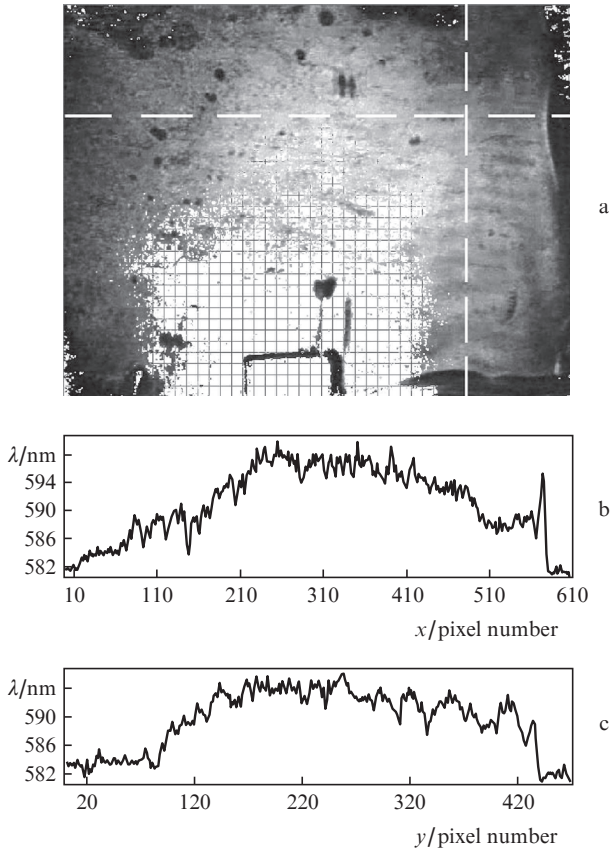

Figure 10. The map of wavelength distribution over image (a) and its horizontal (b) and vertical (c) cross sections for a transient process of holographic layer shrinking. The dashed lines show the cross-section directions.

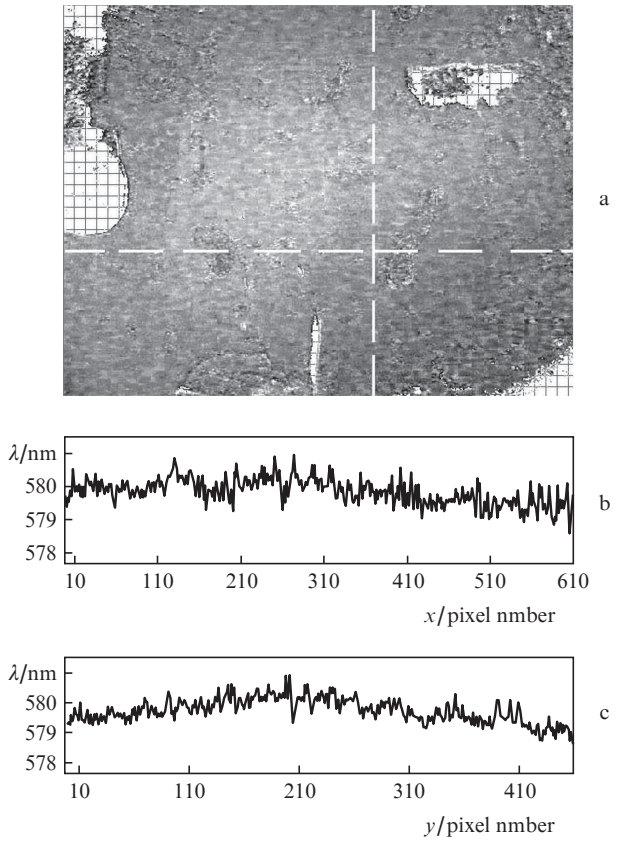

Figure 12. The map of wavelength distribution over image (a) and its horizontal (b) and vertical (c) cross sections for a stationary state of sensor. The dashed lines show the cross-section directions.

of the map are presented at the bottom. One can see that the spread of wavelengths is noticeably reduced as compared to the transient process, and is less than 2 nm over the whole sensor surface. The local spread also strongly reduced and was less than 1 nm. The map comprises approximately 500 000 points.

The hologram quality and uniformity of the processes occurring during swelling can be estimated from their noise characteristics. In Fig. 14, the standard deviation of the calculated wavelengths is shown versus the width of the averaging window. The standard deviation of wavelength from $\bar{\lambda}$

$$A_k = \sqrt{\frac{\sum_i^m (\lambda_i - \bar{\lambda})^2}{m}},$$

where λ_i is the calculated wavelength in the ith pixel of the image and m is the number of points fitting the window, was averaged over N image points covering the whole studied domain of the sensor. The parameter $K = N^{-1}\sum_k^N A_k$ we will term the noise value. Data presented in Fig. 14 correspond to variation of m from 4 to 2500 pixels. The standard deviation was averaged over the image domain of 500×500 points. With

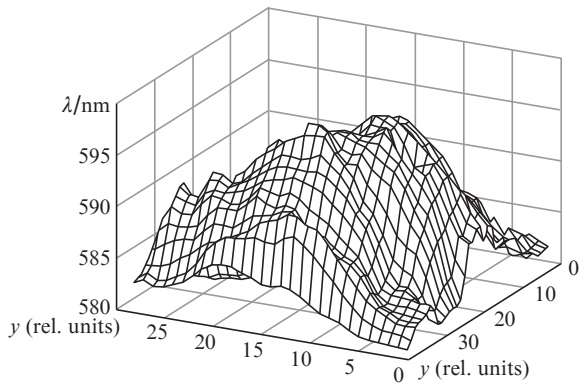

Figure 11. Isometric presentation of the wavelength distribution map (Fig. 10a) in the case of transient shrinking of the holographic layer.

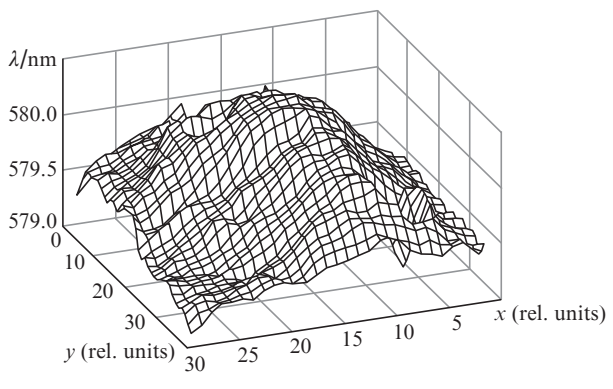

Figure 13. Isometric presentation of the wavelength distribution map (Fig. 12a) for the hologram in a stationary state.

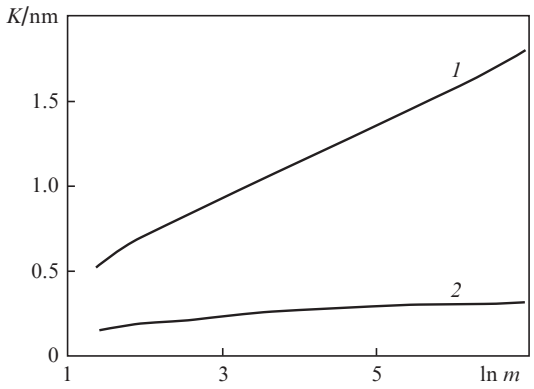

Figure 14. The standard deviation of the calculated wavelength versus the number of points in the averaging window for the transient process (*1*) and stationary sensor state (*2*).

increasing m in the transient process the standard deviation varied from 0.5 to 1.8 nm. A steady increase in noise with the increasing window is related to a large-scale hologram inhomogeneity. In the steady state it was 0.16–0.32 nm at the same values of m. An increase in noise at the initial part of the dependence is explained by small-scale inhomogeneities, and the saturation at large m is related to the absence of large-scale inhomogeneities. The ratio of nonstationary noise to stationary level in this range of m increases from 3.4 to 5.6. These facts bear witness that, first, the hologram in the steady state is highly uniform and, second, variations of its swelling over the surface are noticeably inhomogeneous.

Thus, we suggest the method for measuring the distribution of the average wavelength for narrow-band radiation over the source surface by means of a commercial digital camera. There are the following limitations in using the method: the radiation spectrum should be narrow (the average wavelength is determined); measurements are performed in the spectral range in which at least two sensor types of detecting array are simultaneously sensitive (for the most of cameras studied these ranges are 470–540 nm and 570–600 nm). The accuracy of the determined wavelength is not worse than 1 nm. The method was tested on the yellow doublet of the mercury spectrum and on a continuous spectrum of the incandescent lamp covering the working interval 570–600 nm. By using this method the uniformity of holographic sensor swelling was studied both in a stationary state and in dynamics.

Acknowledgements. This work was supported by a grant within the framework of the Program of Fundamental Studies 'Fundamental Sciences for Medicine' of the Presidium of RAS.

References

1. Kraiskii A.V., Mironova T.V., Sultanov T.T., Postnikov V.A., Sergienko V.I., Tikhonov V.E. S*posob izmereniya dliny volny uzkopolosnogo svetovogo izlucheniya kolorimetricheskim sposobom* (Measuring a Wavelength of Narrow-Band Light Emission by Colorimetric Method), Application to invention of Russian Federation No. 2008119917 from 21.05.2008. The favourable decision from 09.02.2010.
2. Kraiskii A.V., Postnikov V.A., Sultanov T.T., Tikhonov V.E., in *Tez. dokl. konf. 'Fundametal'nye nauki – meditsine'* (Abstracts of Papers of Conference on Fundamental Sciences for Medicine) (Moscow, 2007) p. 79.
3. Kraiskii A.V., Postnikov V.A., Khamidulin A.V., Sultanov T.T. *Kvantovaya Elektron.*, **40**, 178 (2010) [*Quantum. Electron.*, **40**, 178 (2010)].
4. Patent Japan JP 2007 183 218, data publ. 19.07.2007.
5. Patent Germany DE102006032857, data publ. 17.01.2008.
6. Judd D.B., Wyszecki G. *Color in Business, Science and Industry* (New York: Wiley, 1975; Moscow: Mir, 1978).